This is a repository copy of *RARE-based localization for mixed near-field and far-field rectilinear sources*.

White Rose Research Online URL for this paper:
http://eprints.whiterose.ac.uk/143092/

Version: Accepted Version

Article:
Chen, H., Zhu, W.-P., Liu, W. orcid.org/0000-0003-2968-2888 et al. (4 more authors) (2019) RARE-based localization for mixed near-field and far-field rectilinear sources. Digital Signal Processing, 85. pp. 54-61. ISSN 1051-2004

https://doi.org/10.1016/j.dsp.2018.11.006

Article available under the terms of the CC-BY-NC-ND licence (https://creativecommons.org/licenses/by-nc-nd/4.0/).

Reuse
This article is distributed under the terms of the Creative Commons Attribution-NonCommercial-NoDerivs (CC BY-NC-ND) licence. This licence only allows you to download this work and share it with others as long as you credit the authors, but you can't change the article in any way or use it commercially. More information and the full terms of the licence here: https://creativecommons.org/licenses/

Takedown
If you consider content in White Rose Research Online to be in breach of UK law, please notify us by emailing eprints@whiterose.ac.uk including the URL of the record and the reason for the withdrawal request.

White Rose
university consortium
Universities of Leeds, Sheffield & York

eprints@whiterose.ac.uk
https://eprints.whiterose.ac.uk/

*Manuscript
Click here to view linked References

RARE-Based Localization for Mixed Near-Field and Far-Field Rectilinear Sources

Hua Chen[a], Wei-Ping Zhu[b], Wei Liu[c], M.N.S. Swamy[b], Youming Li[a], Qing Wang[d], Zongju Peng[a]

[a] *Faculty of Information Science and Engineering, Ningbo University, Ningbo 315211,P. R. China.*
[b] *Department of Electrical and Computer Engineering, Concordia University, Montreal, QC H3G 1M8, Canada.*
[c] *Department of Electronic and Electrical Engineering, University of Sheffield, Sheffield S1 3JD, UK.*
[d] *School of Electronic Informatin Engineering, Tianjin University, Tianjin 300072, P. R. China.*

Abstract

In this paper, a novel localization method for mixed near-field (NF) and far-field (FF) rectilinear or strictly noncircular sources is proposed using the noncircular information for a symmetric uniform linear array (ULA). For FF case, we adopt the NC-MUSIC method to achieve the DOA parameter, for NF case, by exploiting the center symmetrical characteristic of the ULA, we decouple the array steering vectors into two new vectors: one related only to the DOA parameter, and the other dependent on both DOA and range parameters. Based on the principle of rank reduction (RARE), three MUSIC-like estimators are formed to estimate the direction of arrival (DOA) and the range of mixed NF and FF rectilinear sources successively. Meanwhile, distinguishing the types of sources is also solved. The deterministic Cramer-Rao bound (CRB) of the mixed rectilinear signals is derived by the

Email addresses: dkchenhua0714@hotmail.com (Hua Chen), weiping@ece.concordia.ca (Wei-Ping Zhu), w.liu@sheffield.ac.uk (Wei Liu), swamy@ece.concordia.ca (M.N.S. Swamy)

Slepian-Bangs formulation. Simulation results are provided, showing that the proposed method yields a performance better than existing ones.
Keywords:
DOA estimation, far-field, near-field, rectilinear signals, Cramer-Rao bound (CRB).

---

1. Introduction

Source localization is a fundamental problem in array signal processing, and has found numerous applications in radar, sonar, seismic exploration, and wireless communications, etc.[1–3]. A large number of algorithms have been proposed to deal with the problem in the past decades, and most of them assume far-field (FF) signals, i.e., the direction of arrival (DOA) parameters are estimated based on infinite distance of the sources to the array [4–6]. On the contrary, when the incident sources are located close to the array, i.e. they are near-field (NF) sources, both the DOA and range need to be characterized. Various methods have been developed for NF source localization [7–9]. However, in some practical applications, both NF and FF signals can be present simultaneously, such as speaker localization using microphone arrays and guidance (homing) systems [10]. Thus, the algorithms designed for pure NF or FF sources would lead to inaccurate or unreliable estimation results under such mixed circumstances.

Some recent progress on the estimation of DOA and range parameters of mixed NF and FF sources using the fourth-order cumulant (FOC) was reported in [10–14]. In [10], Liang et al. proposed a two-stage MUSIC algorithm to estimate the DOA and range parameters by constructing two special FOC matrices, one related to the DOA parameter, and the other to

both the DOA and the range. Following the two-stage idea, Wang et al. [11] and Tian et al. [12] presented localization methods for mixed sources based on sparse signal reconstruction. However, method in [12] can detect more mixed sources utilizing symmetric nested array. In [13], a mixed-order MUSIC algorithm based on a sparse symmetric array was proposed, which estimates the DOAs of mixed sources with a cumulant matrix and the range parameters with the traditional covariance matrix. In [14], another mixed-order MUSIC algorithm was proposed, which estimates the DOAs of FF sources with the traditional covariance matrix, and the DOA and range parameters of NF sources with a special cumulant matrix. However, one common issue with these cumulant-based methods is their high computational complexity, and their incapability of dealing with Gaussian sources. Furthermore, for the methods in [10] and [13], the NF and FF sources cannot share the same DOA.

To reduce the computational complexity, a series of second-order statistics (SOS)-based methods were presented in [15–19]. In [15], He et al. proposed a one-dimensional (1-D) MUSIC-based algorithm by resorting to the oblique projection technique to separate the NF and FF sources, which would unfortunately yield extra estimation errors . Then, an alternating iterative method was developed without eigendecomposition to estimate the mixed signals [17], which overcomes the "saturation behavior" in NF localization by recalculating the oblique projector. In [16], ESPRIT-like and polynomial rooting methods were developed to solve the mixed localization problem using the symmetry of the array. In [18], Liu. et al first obtained the DOA and power information of FF sources, and then the NF sources were estimated by eliminating the FF signals information from the signal subspace. With the spatial differencing technique, a method was presented

in [19] to locate the mixed sources by eliminating the FF and noise components, which have a Toeplitz structure, from the covariance matrix of the array observation. However, by these SOS-based methods, the number of the mixed sources that can be estimated is no more than half that of the array elements due to loss of array aperture in the processing.

So far none of the existing methods for localization of mixed NF and FF signals has considered the noncircularity of the impinging signals, which are widely used in modern wireless communication systems, such as PAM and BPSK signals. The estimation accuracy can be improved through expanding the virtual array aperture when the noncircularity property of signals is exploited properly [20–26, 28–30]. Therefore, in this paper, based on a ULA, we propose a localization method for mixed NF and FF sources by exploiting the noncircular information of the signals. Based on the principle of rank reduction (RARE) [31–33], three MUSIC-like estimators are developed to estimate the DOA and range of mixed NF and FF rectilinear sources in a successive way. Meanwhile, distinguishing the types of sources is also solved. Based on the Slepian-Bangs formulation, the deterministic Cramer-Rao bound (CRB) for the mixed NF and FF rectilinear signals is derived as a benchmark.

Notations: $(\cdot)^*$, $(\cdot)^T$, $(\cdot)^H$, and $(\cdot)^{-1}$ represent operations of conjugation, transpose, conjugate transpose, and inverse, respectively; $E[\cdot]$ and $diag\{\cdot\}$ stand for the expectation and diagonalization operations, respectively; $\mathbf{I}_p$ denotes the p-dimensional identity matrix; the $p \times p$ matrix $\mathbf{\Pi}_p$ is an exchange matrix with ones on its anti-diagonal and zeros elsewhere; $blkdiag\{\mathbf{Z}_1, \mathbf{Z}_2\}$ represents a block diagonal matrix with diagonal entries $\mathbf{Z}_1$ and $\mathbf{Z}_2$; $\mathrm{Re}\{\cdot\}$ denotes the real part of a complex number, while $\det\{\cdot\}$ denotes the determinant of a matrix. $\otimes$ and $\odot$ are the kronecker product and Hadamard

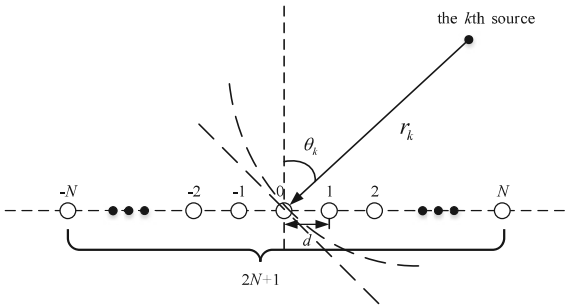

Fig. 1: Uniform linear array configuration.

product operations, respectively.

2. Mixed Far-Field and Near-Field Array Signal Model

Consider a symmetric uniform linear array (ULA) with $M = 2N + 1$ sensors, as shown in Fig.1. There are K uncorrelated narrowband non-circular sources $s_k(l)$ $(k = 1, 2, \ldots, K)$ located in either NF or FF of the array. Without loss of generality, we assume the first K_1 incoming sources $s_{N,k}(l)$ are NF parameterized by (θ_k, r_k) $(k = 1, 2, \ldots, K_1)$, while the remaining $K_2 = K - K_1$ sources $s_{F,k}(l)$ are FF parameterized by (θ_k, ∞) $(k = K_1 + 1, K_1 + 2, \ldots, K)$, and K is known in advance. Let the array center indexed by 0 be the phase reference point. Then the observed noisy signal $x_m(l)$ at sample l $(l = 1, 2, \ldots, L)$ received by the mth $(m = -N, \ldots, 0, \ldots, N)$ sensor can be modeled as [36, 37]

$$\begin{aligned} x_m(l) &= \sum_{k=1}^{K} s_k(l) e^{j\omega_{mk}} + n_m(l) \\ &= \sum_{k=1}^{K_1} s_{N,k}(l) e^{j\frac{2\pi r_k}{\lambda}\left(\sqrt{1+\left(\frac{md}{r_k}\right)^2 - \frac{2md\sin\theta_k}{r_k}} - 1\right)} \\ &\quad + \sum_{k=K_1+1}^{K} s_{F,k}(l) e^{jm\gamma_k} + n_m(l) \end{aligned} \tag{1}$$

where $n_m(l)$ is the additive Gaussian noise with zero mean and variance σ_n^2 at the mth sensor, which is uncorrelated with the impinging signals, and ω_{mk} is the phase offset between the 0th and mth sensors associated with the kth source. For the NF incident signals, ω_{mk} has the form of

$$\omega_{mk} = \frac{2\pi r_k}{\lambda}\left(\sqrt{1+\left(\frac{md}{r_k}\right)^2 - \frac{2md\sin\theta_k}{r_k}} - 1\right) \tag{2}$$

and with second-order expansion, (2) can be expressed as

$$\omega_{mk} \approx m\gamma_k + m^2\chi_k \tag{3}$$

while for the FF ones, we have

$$\omega_{mk} = m\gamma_k \tag{4}$$

where $\gamma_k = -2\pi d sin\theta_k/\lambda$ and $\chi_k = \pi d^2 cos^2\theta_k/(\lambda r_k)$ are called electric angles with λ being the wavelength of the incoming signal, $\theta_k \in \left[-\frac{\pi}{2}, \frac{\pi}{2}\right]$, $k = 1, \cdots K$, the DOA of the kth NF or FF signal, d the spacing between the sensors satisfying $d \leq \lambda/4$ [10] and r_k the range of the kth NF signal that is within the Fresnel region [15] and satisfies $r_k \in \left[0.62(D^3/\lambda)^{1/2}, 2D^2/\lambda\right]$, $k = 1, \cdots K_1$, with D being the array aperture. Thus, (1) can be approximated as

$$\begin{aligned} x_m(l) \approx & \sum_{k=1}^{K_1} s_{N,k}(l)e^{j(m\gamma_k + m^2\chi_k)} \\ & + \sum_{k=K_1+1}^{K} s_{F,k}(l)e^{jm\gamma_k} + n_m(l) \end{aligned} \tag{5}$$

as pointed out in [10], a FF source can be considered as a special NF one where the range r_k approaches to ∞.

By collecting L snapshots of the array output, and arranging them in a matrix form, the received data vector at instant l can be written as

$$\begin{aligned} \mathbf{x}(l) &= [x_{-N}(l), \cdots, x_0(l), \cdots, x_N(l)]^T \\ &= \mathbf{A}\mathbf{s}(l) + \mathbf{n}(l) \end{aligned} \tag{6}$$

where $\mathbf{n}(l)=[n_{-N}(l),\cdots,n_0(l),\cdots,n_N(l)]^T$ represents the circular Gaussian noise vector. Using the partioned forms of $\mathbf{A}$ and $\mathbf{s}(l)$, i.e.,

$$\mathbf{A}=\begin{bmatrix} \mathbf{A}_N & \mathbf{A}_F \end{bmatrix} \tag{7}$$

$$\mathbf{s}(l)=\begin{bmatrix} \mathbf{s}_N^T(l) & \mathbf{s}_F^T(l) \end{bmatrix}^T \tag{8}$$

(6) can be rewritten as

$$\mathbf{x}(l)=\mathbf{A}_N\mathbf{s}_N(l)+\mathbf{A}_F\mathbf{s}_F(l)+\mathbf{n}(l) \tag{9}$$

where $\mathbf{s}_N(l)$ and $\mathbf{s}_F(l)$ are the signal vectors of NF and that of FF sources, respectively, and $\mathbf{A}_N$ and $\mathbf{A}_F$ are the array steering matrix of NF and FF signals with $\mathbf{a}_N(\theta_k,r_k)$ and $\mathbf{a}_F(\theta_k)$ representing respectively the NF and the FF steering vectors, i.e.,

$$\mathbf{A}_N=[\mathbf{a}_N(\theta_1,r_1),\cdots,\mathbf{a}_N(\theta_{K_1},r_{K_1})] \tag{10}$$

$$\begin{aligned}\mathbf{A}_F&=[\mathbf{a}_N(\theta_{K_1+1},\infty),\cdots,\mathbf{a}_N(\theta_K,\infty)]\\&=[\mathbf{a}_F(\theta_{K_1+1}),\cdots,\mathbf{a}_F(\theta_K)]\end{aligned} \tag{11}$$

with $\mathbf{a}_N(\theta_k,r_k)=[e^{j(-N\gamma_k+N^2\chi_k)},\cdots,1,\cdots,e^{j(N\gamma_k+N^2\chi_k)}]^T$,
$\mathbf{a}_F(\theta_k)=[e^{j(-N\gamma_k)},\cdots,1,\cdots,e^{j(N\gamma_k)}]^T$.

Due to the rectilinearity of the sources, which can be modeled as the product of a complex scalar $e^{-j\psi/2}$ and a real valued signal $s_0(t)$, the signal vectors $\mathbf{s}_N(l)$ and $\mathbf{s}_F(l)$ can be expressed as [26–29]

$$\mathbf{s}_N(l)=\boldsymbol{\psi}_{No}^{1/2}\mathbf{s}_{No}(l) \tag{12}$$

$$\mathbf{s}_F(l)=\boldsymbol{\psi}_{Fo}^{1/2}\mathbf{s}_{Fo}(l) \tag{13}$$

where $\mathbf{s}_{No}(l)=[s_{o,1}(l),\cdots,s_{o,K_1}(l)]^T$ and $\mathbf{s}_{Fo}(l)=[s_{o,K_1+1}(l),\cdots,s_{o,K}(l)]^T$ are the NF and FF real-valued signals, respectively. The diagonal matrices

$\boldsymbol{\psi}_{No}^{1/2} = diag(e^{j\psi_1/2}, \cdots, e^{j\psi_{K_1}/2})$ and $\boldsymbol{\psi}_{Fo}^{1/2} = diag(e^{j\psi_{K_1+1}/2}, \cdots, e^{j\psi_K/2})$ are the arbitrary phase shifts corresponding to the NF and FF strictly noncircular sources $\mathbf{s}_N(l)$ and $\mathbf{s}_F(l)$, respectively.

3. The Proposed Method

In this section, we develop a two-stage RARE-based localization method to determine the DOAs $(\theta_k, k = 1, 2, \cdots, K)$ and ranges $(r_k, k = 1, 2, \cdots, K_1)$ of the mixed NF and FF strictly noncircular sources.

In order to exploit the noncircular information of the mixed incident signals, we construct a new vector $\mathbf{z}(l)$ by stacking the observed data vector $\mathbf{x}(l)$ and its conjugate counterpart $\mathbf{x}^*(l)$ as follows

$$\begin{aligned}\mathbf{z}(l) &= \begin{bmatrix} \mathbf{x}(l) \\ \mathbf{x}^*(l) \end{bmatrix} \\ &= \mathbf{A}_{eN}\mathbf{s}_N(l) + \mathbf{A}_{eF}\mathbf{s}_F(l) + \mathbf{n}_e(l) \\ &= \mathbf{A}_e\mathbf{s}(l) + \mathbf{n}_e(l)\end{aligned} \tag{14}$$

where

$$\mathbf{A}_e = \begin{bmatrix} \mathbf{A}_{eN} & \mathbf{A}_{eF} \end{bmatrix} \tag{15}$$

with

$$\mathbf{A}_{eN} = \begin{bmatrix} \mathbf{A}_N \\ \mathbf{A}_N{}^*\boldsymbol{\psi}_N{}^* \end{bmatrix} = [\mathbf{a}_{eN}(\theta_1, r_1, \psi_1), \cdots, \mathbf{a}_{eN}(\theta_{K_1}, r_{K_1}, \psi_{K_1})] \tag{16}$$

$$\mathbf{a}_{eN}(\theta_k, r_k, \psi_k) = \begin{bmatrix} \mathbf{a}_N(\theta_k, r_k) \\ \mathbf{a}_N{}^*(\theta_k, r_k)e^{-j\psi_k} \end{bmatrix} \tag{17}$$

$$\begin{aligned}\mathbf{A}_{eF} &= \begin{bmatrix} \mathbf{A}_F \\ \mathbf{A}_F{}^*\boldsymbol{\psi}_F{}^* \end{bmatrix} \\ &= [\mathbf{a}_{eF}(\theta_{K_1+1}, \psi_{K_1+1}), \cdots, \mathbf{a}_{eF}(\theta_K, \psi_K)]\end{aligned} \tag{18}$$

$$\mathbf{a}_{eF}(\theta_k, \psi_k) = \begin{bmatrix} \mathbf{a}_F(\theta_k) \\ \mathbf{a}_F{}^*(\theta_k) e^{-j\psi_k} \end{bmatrix} \tag{19}$$

$$\mathbf{n}_e(l) = \begin{bmatrix} \mathbf{n}(l) \\ \mathbf{n}^*(l) \end{bmatrix} \tag{20}$$

Using (17) and (19) into (15), we obtain the steering vector $\mathbf{a}_e$ of $\mathbf{A}_e$ as follows,

$$\mathbf{a}_e(\theta_k, r_k, \psi_k) = \begin{bmatrix} \mathbf{a}(\theta_k, r_k) \\ \mathbf{a}^*(\theta_k, r_k) e^{-j\psi_k} \end{bmatrix} \tag{21}$$

with

$$\mathbf{a}(\theta_k, r_k) = [e^{j(-N\gamma_k + N^2\chi_k)}, \cdots, 1, \cdots, e^{j(N\gamma_k + N^2\chi_k)}]^T \tag{22}$$

$k = 1, \cdots, K$, $r_k \in \left[0.62(D^3/\lambda)^{1/2}, +\infty\right)$.

The covariance matrix of $\mathbf{z}(l)$ is

$$\begin{aligned} \mathbf{R} &= E[\mathbf{z}(l)\mathbf{z}^H(l)] \\ &= \mathbf{A}_e \mathbf{R}_s \mathbf{A}_e^H + \sigma_n^2 \mathbf{I}_{2M} \\ &= \mathbf{A}_{eN} \mathbf{R}_{sN} \mathbf{A}_{eN}^H + \mathbf{A}_{eF} \mathbf{R}_{sF} \mathbf{A}_{eF}^H + \sigma_n^2 \mathbf{I}_{2M} \\ &= \mathbf{R}_N + \mathbf{R}_F + \sigma_n^2 \mathbf{I}_{2M} \end{aligned} \tag{23}$$

where $\mathbf{R}_{sN} = E[\mathbf{s}_N(l)\mathbf{s}_N^H(l)]$, $\mathbf{R}_{sF} = E[\mathbf{s}_F(l)\mathbf{s}_F^H(l)]$ and $\mathbf{R}_s = E[\mathbf{s}(l)\mathbf{s}^H(l)]$ are the covariance matrices of NF, FF and total mixed signals, respectively. The eigenvalue decomposition of $\mathbf{R}$ is given by

$$\mathbf{R} = \mathbf{U}_s \mathbf{\Lambda}_s \mathbf{U}_s^H + \mathbf{U}_n \mathbf{\Lambda}_n \mathbf{U}_n^H \tag{24}$$

where the $2M \times K$ matrix $\mathbf{U}_s$ and the $2M \times (2M - K)$ matrix $\mathbf{U}_n$ are the signal subspace and noise subspace, respectively. The $K \times K$ matrix $\mathbf{\Lambda}_s = diag\{\lambda_1, \lambda_2, \ldots, \lambda_K\}$ and the $(2M - K) \times (2M - K)$ matrix $\mathbf{\Lambda}_n = diag\{\lambda_{K+1}, \lambda_{K+2}, \ldots, \lambda_{2M}\}$ are diagonal matrices, where $\lambda_1 \geq \lambda_2 \geq \cdots \geq \lambda_K > \lambda_{K+1} = \cdots = \lambda_{2M} = \sigma_n^2$ are the eigenvalues of $\mathbf{R}$.

3.1. DOA Estimation of FF Sources

Based on the orthogonality between $\mathbf{U}_n$ and $\mathbf{a}_{eF}(\theta_{k_F}, \psi_{k_F})$, the following result can be obtained

$$\begin{aligned}\mathbf{U}_n^H \mathbf{a}_{eF}(\theta_k, \psi_k) &= \mathbf{U}_n^H \begin{bmatrix} \mathbf{a}_F(\theta_k) \\ \mathbf{a}_F{}^*(\theta_k) e^{-j\psi_k} \end{bmatrix} \\ &= \mathbf{U}_n^H \ \ blkdiag\{\mathbf{a}_F(\theta_k), \mathbf{a}_F^*(\theta_k)\} \begin{bmatrix} 1 \\ e^{-j\psi_{k_F}} \end{bmatrix} = \mathbf{0}\end{aligned} \tag{25}$$

Therefore, we can construct the estimator of θ for far-field sources as follows

$$p_F(\theta) = \{\det[\mathbf{Q}_F(\theta)]\}^{-1}. \tag{26}$$

where $\mathbf{Q}_F(\theta) = \mathbf{V}_F^H(\theta)\mathbf{U}_n\mathbf{U}_n^H\mathbf{V}_F(\theta)$ with $\mathbf{V}_F(\theta) = \ \ blkdiag\{\mathbf{a}_F(\theta), \mathbf{a}_F^*(\theta)\}$. Based on the RARE principle where the required uniqueness condition ensures that the considered matrix drops rank (More details about RARE can be found in [31–33]), the $(4N + 2 - K) \times 2$ dimension matrix $\mathbf{U}_n^H\mathbf{V}_F(\theta)$ should be of full column rank, satisfying the condition $(4N+2-K) \geq 2$, i.e. $K \leq 4N$, and then if and only if $\theta = \theta_k$, the matrix $\mathbf{Q}_F(\theta)$ becomes rank deficient or equivalently $\det[\mathbf{Q}_F(\theta)] = 0$. By searching over the range of $\theta \in \left[-\frac{\pi}{2}, \frac{\pi}{2}\right]$, the DOAs of far-field sources can be obtained from the peaks of $p_F(\theta)$.

3.2. DOA Estimation of NF Sources and Identification Types of Sources

Since the array is center symmetric about the 0th sensor, (22) can be rewritten as [7, 16]

$$\mathbf{a}(\theta_k, r_k) = \mathbf{K}(\theta_k)\boldsymbol{\varsigma}(\theta_k, r_k) \tag{27}$$

where $\mathbf{K}(\theta_k)$ is a $(2N + 1) \times (N + 1)$ matrix, whose elements depend only on the DOA parameter, i.e.,

$$\mathbf{K}(\theta_k) = \begin{bmatrix} \mathbf{V}_1^T(\theta_k) & \mathbf{v}_2^T(\theta_k) & \mathbf{V}_3^T(\theta_k) \end{bmatrix}^T \tag{28}$$

where

$$\mathbf{V}_1(\theta_k) = [\mathbf{P}_1(\theta_k), \mathbf{0}_{N\times 1}]_{N\times(N+1)} \tag{29}$$

with

$$\mathbf{P}_1(\theta_k) = diag\{e^{j(-N)\gamma_k}, e^{j(-N+1)\gamma_k}, ..., e^{-j\gamma_k}\} \tag{30}$$

$$\mathbf{v}_2(\theta_k) = [0, \ldots, 0, 1]_{1\times(N+1)} \tag{31}$$

$$\mathbf{V}_3(\theta_k) = [\mathbf{\Pi}_N \mathbf{P}_3(\theta_k), \mathbf{0}_{N\times 1}]_{N\times(N+1)} \tag{32}$$

with

$$\mathbf{P}_3(\theta_k) = diag\{e^{j(N)\gamma_k}, e^{j(N-1)\gamma_k}, ..., e^{j\gamma_k}\} \tag{33}$$

where $\mathbf{P}_1(\theta_k)$ denotes the diagonalization of the steering vector related to the left side of the 0th sensor from the $-N$th to the-1th sensor, and $\mathbf{P}_3(\theta_k)$ denotes the anti-diagonalization of the steering vector related to the right side of the 0th sensor from the 1th to the Nth sensor.

Meanwhile, $\boldsymbol{\varsigma}(\theta_k, r_k)$ is dependent on both the DOA and range parameters as given by

$$\boldsymbol{\varsigma}(\theta_k, r_k) = [e^{j(-N)^2\chi_k}, e^{j(-N+1)^2\chi_k}, ..., 1]^T \tag{34}$$

Based on the orthogonality between $\mathbf{U}_n$ and $\mathbf{a}_e(\theta, r, \psi)$, the following three-dimensional (3-D) scalar pseudo-spectrum function can be obtained:

$$g(\theta, r, \psi) = [\mathbf{a}_e^H(\theta, r, \psi)\mathbf{U}_n\mathbf{U}_n^H\mathbf{a}_e(\theta, r, \psi)]^{-1} \tag{35}$$

Via a 3-D peak-spectrum search, the NF strictly noncircular signals can be located. However, the exhaustive search process is very time-consuming with extremely high computational cost. To avoid the 3-D search, we present a two-stage RARE-based MUSIC algorithm for both DOA and range estimation through two one-dimensional (1-D) searches. Based on the principle

of RARE, the DOAs of the NF signals are obtained by 1-D peak spectrum search. Next, with the estimated DOAs of all incoming signals, another estimator is constructed to find the range parameter using the RARE principle again.

By left-multiplying (21) with $\mathbf{U}_n^H$, and using (27), we have

$$\begin{aligned}\mathbf{0} = &\ \mathbf{U}_n^H \mathbf{a}_e(\theta_k, r_k, \psi_k) \\ =&\mathbf{U}_n^H \boldsymbol{\upsilon}(\theta_k)\boldsymbol{\zeta}(\theta_k, r_k)\boldsymbol{\iota}(\psi_k)\end{aligned} \tag{36}$$

where

$$\boldsymbol{\upsilon}(\theta_k)=blkdiag\{\boldsymbol{\kappa}(\theta_k), \boldsymbol{\kappa}^*(\theta_k)\} \tag{37}$$

$$\boldsymbol{\zeta}(\theta_k, r_k)=blkdiag\{\boldsymbol{\varsigma}(\theta_k, r_k), \boldsymbol{\varsigma}^*(\theta_k, r_k)\} \tag{38}$$

$$\boldsymbol{\iota}(\psi_k)=\begin{bmatrix} 1 \\ e^{-j\psi_k} \end{bmatrix} \tag{39}$$

We now define a function $p(\theta)$ that is related only to the DOA parameter as follows

$$p(\theta) = \{\det[\mathbf{Q}_1(\theta)]\}^{-1}. \tag{40}$$

where $\mathbf{Q}_1(\theta) = \boldsymbol{\upsilon}^H(\theta)\mathbf{U}_n\mathbf{U}_n^H\boldsymbol{\upsilon}(\theta)$. Note that $\boldsymbol{\zeta}(\theta_k, r_k) \neq \mathbf{0}$, $\boldsymbol{\iota}(\psi_k) \neq \mathbf{0}$, and $\mathbf{U}_n^H\boldsymbol{\upsilon}(\theta_k)\boldsymbol{\zeta}(\theta_k, r_k)\boldsymbol{\iota}(\psi_k) = \mathbf{0}, k = 1, 2 \ldots K$. Based on the RARE principle, the $(4N + 2 - K) \times (2N + 2)$ dimension matrix $\mathbf{U}_n^H\boldsymbol{\upsilon}(\theta)$ should be of full column rank, satisfying the condition $(4N + 2 - K) \geq (2N + 2)$, i.e. $K \leq 2N$, and then if and only if $\theta = \theta_k$, the matrix $\mathbf{Q}_1(\theta)$ is rank deficient or equivalently $\det[\mathbf{Q}_1(\theta)] = 0$. If searched over the confined region $\theta \in \left[-\frac{\pi}{2}, \frac{\pi}{2}\right]$, the DOAs θ_k of all NF signals can be obtained from the peaks of $p(\theta)$.

Here, it should be pointed out that the estimator (40) can also be adopted for FF signals, and when some of the NF signals have the same DOAs as the FF signals do, we only get K' DOAs with $K' \leq K$.

3.3. Range Estimation of NF Sources

First, we substitute the achieved θ from (40) into (36) and obtain the following function of the range parameter r:

$$p'(r) = \{\det[\mathbf{Q}_2(\theta, r)]\}^{-1}. \tag{41}$$

where $\mathbf{Q}_2(\theta, r) = \boldsymbol{\zeta}^H(\theta, r)\boldsymbol{\upsilon}^H(\theta)\mathbf{U}_n\mathbf{U}_n^H\boldsymbol{\upsilon}(\theta)\boldsymbol{\zeta}(\theta, r)$. Similarly, the condition $K \leq 4N$ should be satisfied for $\mathbf{Q}_2(\theta, r)$ using the RARE criterion. Again, by searching the range $r \in \left[0.62(D^3/\lambda)^{1/2}, 2D^2/\lambda\right)$, the corresponding range of the mixed signals can be obtained from the peaks of $p'(r)$. At this point, the paired DOA and range parameters (θ and r) can be automatically obtained without any additional operation. The proposed method is summarized in Table 1.

Table 1: Summary of the proposed method.

Input: L snapshots of the new constructed array output vector, $\{\mathbf{z}(t)\}_{l=1}^{L}$.
Output: DOA and range estimates of all mixed NF and FF signals, $\hat{\theta}_k$ and $\hat{r}_k$.
Step 1 Estimate the covariance matrix $\hat{\mathbf{R}} = \frac{1}{L}\sum_{l=1}^{L}\mathbf{z}(l)\mathbf{z}^H(l)$.
Step 2 Perform subspace decomposition $\hat{\mathbf{R}} = \hat{\mathbf{U}}_s\hat{\mathbf{\Lambda}}_s\hat{\mathbf{U}}_s^H + \hat{\mathbf{U}}_n\hat{\mathbf{\Lambda}}_n\hat{\mathbf{U}}_n^H$ to get $\hat{\mathbf{U}}_n$.
Step 3 Construct and search $p_F(\theta)$ to obtain all DOAs $\hat{\theta}_k$ of FF signals with (26).
Step 4 Construct and search $p(\theta)$ to obtain all DOAs $\hat{\theta}_k$ of NF signals with (40).
Step 5 Construct and search $p'(r)$ to obtain all ranges $\hat{r}_k$ of NF signals with the estimated $\hat{\theta}_k$ with (41).

Remark 1: In practice, only a finite number of observed data samples is available. Thus, $\mathbf{R}$ has to be estimated by

$$\hat{\mathbf{R}} = \frac{1}{L}\sum_{l=1}^{L}\mathbf{z}(l)\mathbf{z}^H(l). \tag{42}$$

Remark 2: In [34], Xie. et al have demonstrated that the maximum number of identifiable mixed signals of the existing methods [15–19] is N for a $2N+1$ ULA. For the proposed method, this number is $2N$, twice that of the existing methods due to the use of noncircular information of the mixed signals.

Remark 3: It is of interest to conduct complexity analysis in terms of the number of complex-valued multiplications for the proposed method including the construction of $\hat{\mathbf{R}}$, performing EVD of $\hat{\mathbf{R}}$, the determinant calculation in the RARE step and spectral searching. The complexity of He's method in [15], Jiang's method in [16], Zuo's method in [17], and Liu's method in [18] are also compared. To calculate $\hat{\mathbf{R}}$, $(2M)^2L$ flops are needed. The computational complexity of the EVD on the covariance matrix $\hat{\mathbf{R}}$ is roughly $(2M)^3$ flops. The computational complexity of three determinant calculations is $[8+(2N+2)^3]\frac{\pi}{\triangle\theta}+8\frac{2D^2/\lambda-0.62(D^3/\lambda)^{1/2}}{\triangle r}$ flops. Define the scanning interval of $\theta\in\left[-\frac{\pi}{2},\frac{\pi}{2}\right]$ with a stepsize $\triangle\theta$, and that of $r\in\left[0.62(D^3/\lambda)^{1/2},2D^2/\lambda\right]$ with a stepsize $\triangle r$. The proposed method employs three 1-D spatial spectrum searching procedures to obtain the DOA and range of mixed signals, which has a computational complexity of $(2\frac{\pi}{\triangle\theta}(2M)^2+K_1\frac{2D^2/\lambda-0.62(D^3/\lambda)^{1/2}}{\triangle r}(2M)^2)$ flops, while a direct 3-D spatial spectrum search entails a computational complexity of $\frac{\pi}{\triangle\theta}\frac{2\pi}{\triangle\psi}\frac{2D^2/\lambda-0.62(D^3/\lambda)^{1/2}}{\triangle r}(2M)^2$ flops, where $\psi\in[0,2\pi]$ with a stepsize $\triangle\psi$. For He'smethod, it is about $M^2L+(N+2)^2N+M^3+(N+2)^3+\frac{\pi}{\triangle\theta}(N+2)^2+\frac{\pi}{\triangle\theta}M^2+K_1\frac{2D^2/\lambda-0.62(D^3/\lambda)^{1/2}}{\triangle r}M^2$ flops; for Jiang's method, it is $M^2L+M^3+(2N)^3\frac{\pi}{\triangle\theta}+2NK+K'(2M+1)K$ flops; for Zuo's method, we have $M^2L+3M^3+M^2+\frac{\pi}{\triangle\theta}(N+1)^2+\frac{\pi}{\triangle\theta}M^2+K_1\frac{2D^2/\lambda-0.62(D^3/\lambda)^{1/2}}{\triangle r}M^2$ flops; Liu's method in [18] has a complexity of $M^2L+2M^3+(2N)^3\frac{\pi}{\triangle\theta}+$

$\frac{\pi}{\triangle\theta}(2N)^2 + \frac{\pi}{\triangle\theta}M^2 + K_1\frac{2D^2/\lambda - 0.62(D^3/\lambda)^{1/2}}{\triangle r}M^2$ flops. Obviously, the computational complexity of the proposed method is higher than methods in [15–18] due to the operations associated with the extended covariance matrix; however, the proposed method based on the three 1-D spatial spectrum searching procedures is more computationally efficient than the direct 3-D operation for dense stepsizes $\triangle\theta, \triangle\beta$ and $\triangle\psi$ to achieve better estimation performance. The computational complexity comparison for these methods is summarized in Table 2.

Table 2: Computational complexity comparison for different methods.

Methods	Computational complexity (flops)
He [15]	$M^2L + (N+2)^2N + M^3 + (N+2)^3 + \frac{\pi}{\triangle\theta}(N+2)^2 + \frac{\pi}{\triangle\theta}M^2$ $+K_1\frac{2D^2/\lambda - 0.62(D^3/\lambda)^{1/2}}{\triangle r}M^2$
Jiang [16]	$M^2L + M^3 + (2N)^3\frac{\pi}{\triangle\theta} + 2NK + K'(2M+1)K$
Zuo [17]	$M^2L + 3M^3 + M^2 + \frac{\pi}{\triangle\theta}(N+1)^2 + \frac{\pi}{\triangle\theta}M^2$ $+K_1\frac{2D^2/\lambda - 0.62(D^3/\lambda)^{1/2}}{\triangle r}M^2$
Liu [18]	$M^2L + 2M^3 + (2N)^3\frac{\pi}{\triangle\theta} + \frac{\pi}{\triangle\theta}(2N)^2 + \frac{\pi}{\triangle\theta}M^2$ $+K_1\frac{2D^2/\lambda - 0.62(D^3/\lambda)^{1/2}}{\triangle r}M^2$
Proposed	$(2M)^2L + (2M)^3 + [8 + (2N+2)^3]\frac{\pi}{\triangle\theta} + 8\frac{2D^2/\lambda - 0.62(D^3/\lambda)^{1/2}}{\triangle r}$ $+[2\frac{\pi}{\triangle\theta}(2M)^2 + K_1\frac{2D^2/\lambda - 0.62(D^3/\lambda)^{1/2}}{\triangle r}(2M)^2]$
MD searching	$(2M)^2L + (2M)^3 + \frac{\pi}{\triangle\theta}\frac{2\pi}{\triangle\psi}\frac{2D^2/\lambda - 0.62(D^3/\lambda)^{1/2}}{\triangle r}(2M)^2$

Remark 4: Due to several 1-D spatial spectrum searching procedures required in the proposed method, we can also use the computationally cheap root-MUSIC method to estimate the DOA and range parameters to reduce the complexity.

Remark 5: The proposed method cannot directly be applied to non-rectilinear sources (general noncircular sources), because non-rectilinear sources do not have the extended array steering matrix structure in Eqs.(13) and (16), and thus the orthogonality between the extended array steering vector and noise subspaces can not be ensured. Therefore, we need to revise the proposed method by referring to the method in [35], which is beyond the scope of this manuscript, and will be a topic of research in our further work.

4. Deterministic rectilinear CRB

In this section, we analyze the deterministic CRB of the estimates of DOA and range parameters of mixed NF and FF rectilinear signals. With the deterministic data assumption, we would like to derive a closed-form expression of the deterministic CRB for both DOA and range parameters of mixed sources, as an estimation benchmark for the scenario with mixed NF and FF rectilinear signals. The derivation is based on the Slepian-Bangs formula, and the result is summarized in the following.

First, we have to specify the parameters of the Gaussian distribution of $\tilde{\mathbf{z}}(l)$ in (14) with exact NF model [36, 37] in (1). Define a real-valued vector of the unknown parameters as $\boldsymbol{\xi} = \begin{bmatrix} \boldsymbol{\theta}_N^T & \mathbf{r}_N^T & \boldsymbol{\Psi}_N^T & \boldsymbol{\theta}_F^T & \boldsymbol{\Psi}_F^T \end{bmatrix}^T$. with $\boldsymbol{\theta}_N = [\theta_1, \theta_2, ..., \theta_{K_1}]^T$, $\mathbf{r}_N = [r_1, r_2, ..., r_{K_1}]^T$, $\boldsymbol{\Psi}_N = [\psi_1, ..., \psi_{K_1}]^T$, $\boldsymbol{\theta}_F = [\theta_{K_1+1}, \theta_{K_1+2}, ..., \theta_K]^T$, and $\boldsymbol{\Psi}_F = [\psi_{K_1+1}, ..., \psi_K]^T$.

Then, the (p, q)th entry of the $(3K_1 + 2K_2) \times (3K_1 + 2K_2)$ CRB matrix for the parameter $\boldsymbol{\xi}$ estimates is given by [38]

$$[\mathrm{CRB}^{-1}(\boldsymbol{\xi})]_{p,q} = \frac{L}{\sigma^2} \mathrm{Re} \left\{ \frac{\partial \tilde{\mathbf{A}}_e^{\mathrm{H}}}{\partial \boldsymbol{\xi}_{\mathrm{p}}} \mathbf{P}_{\tilde{\mathbf{A}}_e}^{\perp} \frac{\partial \tilde{\mathbf{A}}_e}{\partial \boldsymbol{\xi}_{\mathrm{q}}} \mathbf{P}_{\mathrm{s}} \right\} \tag{43}$$

where $\tilde{\mathbf{A}}_e$ denotes the extended steering matrix (15) with exact NF model, $\mathbf{P}^{\perp}_{\tilde{\mathbf{A}}_e} = \mathbf{I}_{4N+2} - \tilde{\mathbf{A}}_e(\tilde{\mathbf{A}}_e^H \tilde{\mathbf{A}}_e)^{-1}\tilde{\mathbf{A}}_e^H$, $\mathbf{P}_s = E[\mathbf{s}(l)\mathbf{s}^H(l)] \in C^{K\times K}$.

Define

$$\tilde{\mathbf{D}}_{eN} = \left[\frac{\partial \tilde{\mathbf{A}}_e}{\partial \theta_1}, ..., \frac{\partial \tilde{\mathbf{A}}_e}{\partial \theta_{K_1}}, \frac{\partial \tilde{\mathbf{A}}_e}{\partial r_1}, ..., \frac{\partial \tilde{\mathbf{A}}_e}{\partial r_{K_1}}, \frac{\partial \tilde{\mathbf{A}}_e}{\partial \psi_1}, ..., \frac{\partial \tilde{\mathbf{A}}_e}{\partial \psi_{K_1}}, \mathbf{0}_{2M\times 2K_2}\right] \tag{44}$$

$$\tilde{\mathbf{D}}_{eF} = \left[\mathbf{0}_{2M\times 3K_1}, \frac{\partial \tilde{\mathbf{A}}_e}{\partial \theta_{K_1+1}}, ..., \frac{\partial \tilde{\mathbf{A}}_e}{\partial \theta_K}, \frac{\partial \tilde{\mathbf{A}}_e}{\partial \psi_{K_1+1}}, ..., \frac{\partial \tilde{\mathbf{A}}_e}{\partial \psi_K}\right] \tag{45}$$

and further partition the matrix $\mathbf{P}_s$ into four matrices $\mathbf{P}_{s1} \in C^{K_1\times K_1}$, $\mathbf{P}_{s2} \in C^{K_1\times K_2}$, $\mathbf{P}_{s3} \in C^{K_2\times K_1}$ and $\mathbf{P}_{s4} \in C^{K_2\times K_2}$ as follows

$$\mathbf{P}_s = \begin{bmatrix} \mathbf{P}_{s1} & \mathbf{P}_{s2} \\ \mathbf{P}_{s3} & \mathbf{P}_{s4} \end{bmatrix}. \tag{46}$$

After some simplification, we derive the closed-form expression for the CRB $\boldsymbol{\xi}$ as

$$\mathrm{CRB}(\boldsymbol{\xi}) = \frac{\sigma^2}{L}\begin{bmatrix} \mathrm{CRB}_1(\boldsymbol{\xi}) & \mathrm{CRB}_2(\boldsymbol{\xi}) \\ \mathrm{CRB}_3(\boldsymbol{\xi}) & \mathrm{CRB}_4(\boldsymbol{\xi}) \end{bmatrix}^{-1} \tag{47}$$

where

$$\mathrm{CRB}_1(\boldsymbol{\xi}) = \left\{\mathrm{Re}[(\mathbf{J}_N(\tilde{\mathbf{D}}_{eN}^H \mathbf{P}^{\perp}_{\tilde{\mathbf{A}}_e}\tilde{\mathbf{D}}_{eN})\mathbf{J}_N^T) \odot (\mathbf{1}_3 \otimes \mathbf{1}_3^T \otimes \mathbf{P}_{s1}^T)]\right\}^{-1} \tag{48}$$

$$\mathrm{CRB}_2(\boldsymbol{\xi}) = \left\{\mathrm{Re}[(\mathbf{J}_N(\tilde{\mathbf{D}}_{eN}^H \mathbf{P}^{\perp}_{\tilde{\mathbf{A}}_e}\tilde{\mathbf{D}}_{eF})\mathbf{J}_F^T) \odot (\mathbf{1}_2 \otimes \mathbf{1}_3^T \otimes \mathbf{P}_{s3}^T)]\right\}^{-1} \tag{49}$$

$$\mathrm{CRB}_3(\boldsymbol{\xi}) = \left\{\mathrm{Re}[(\mathbf{J}_F(\tilde{\mathbf{D}}_{eF}^H \mathbf{P}^{\perp}_{\tilde{\mathbf{A}}_e}\tilde{\mathbf{D}}_{eN})\mathbf{J}_N^T) \odot (\mathbf{1}_3 \otimes \mathbf{1}_2^T \otimes \mathbf{P}_{s2}^T)]\right\}^{-1} \tag{50}$$

$$\mathrm{CRB}_4(\boldsymbol{\xi}) = \left\{\mathrm{Re}[(\mathbf{J}_F(\tilde{\mathbf{D}}_{eF}^H \mathbf{P}^{\perp}_{\tilde{\mathbf{A}}_e}\tilde{\mathbf{D}}_{eF})\mathbf{J}_F^T) \odot (\mathbf{1}_2 \otimes \mathbf{1}_2^T \otimes \mathbf{P}_{s4}^T)]\right\}^{-1} \tag{51}$$

with $\mathbf{J}_N = [\mathbf{I}_{3K_1}, \mathbf{0}_{3K_1\times 2K_2}]$, $\mathbf{J}_F = [\mathbf{0}_{2K_2\times 3K_1}, \mathbf{I}_{2K_2}]$, $\mathbf{1}_3 = [1,1,1]$ and $\mathbf{1}_2 = [1,1]$.

It is noted that when all the sources are NF sources, we have $\mathrm{CRB}(\boldsymbol{\xi}) = \mathrm{CRB}_1(\boldsymbol{\xi})$, and when all the sources are FF sources, $\mathrm{CRB}(\boldsymbol{\xi}) = \mathrm{CRB}_4(\boldsymbol{\xi})$.

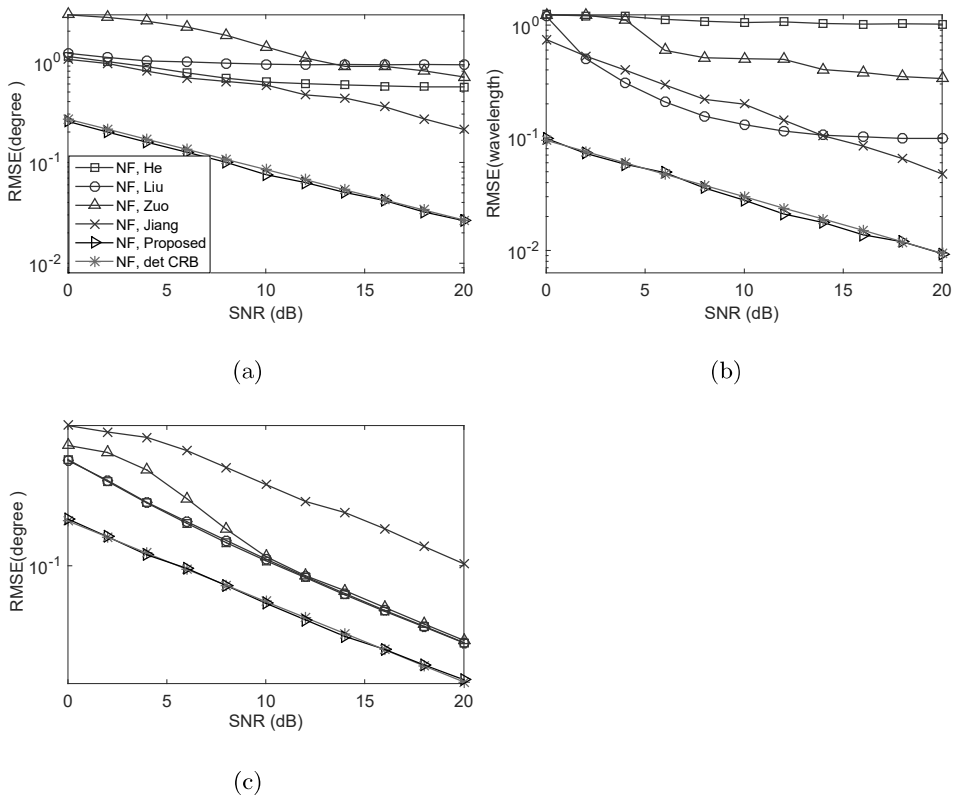

Fig. 2: RMSE of two NF and two FF sources versus SNR with snapshots number to be 500. (a) NF angle estimation. (b) NF range estimation. (c) FF angle estimation.

5. Simulation Results

In this section, computer simulation is conducted to demonstrate the experimental and theoretical results of the proposed method as compared with some of the existing methods including He's method [15], Jiang's method [16], Zuo's method [17], Liu's method [18] and deterministic CRB in (47) for the scenario of mixed NF and FF rectilinear sources. For the first and second sets of simulations, a ULA of 9 sensors ($N = 4$) with a quarter-wavelength inter-sensor spacing ($d = \lambda/4$) is employed, while for the third simulation, a ULA of 5 sensors ($N = 2$) is used. The impinging sources are equi-power, uncorrelated BPSK signals, and the additive noise is assumed to be spatial white complex Gaussian, and the SNR is defined relative to each signal. The root mean square error (RMSE) $\mathrm{RMSE}(\vartheta_{K_i}) = \sqrt{\frac{1}{K_i M_c}\sum_{k=1}^{K_i}\sum_{q=1}^{M_c}\left(\hat{\vartheta}_{qk} - \vartheta_k\right)^2}$, $K_i = K_1, K_2$, is adopted for quantitative evaluation, where M_c is the number of Monte Carlo simulations, K_i is the number of NF or FF signals, $\hat{\vartheta}_{q,k}$ is the estimate of the parameter $\hat{\theta}_k$ or $\hat{r}_k$ in the kth Monte Carlo simulation, and ϑ_k is the true value standing for either θ_k or r_k. The results of the first and second sets of simulations are obtained from 500 independent Monte Carlo trials, while that of the third one is from 20 independent Monte Carlo trials.

In the first set of simulations, two NF sources and two FF sources impinge upon the above nine-sensor ULA, and we examine the performance of the proposed method in comparison with the existing methods versus the SNR. Two NF signals are located at $(5^\circ + v_1, 1.9\lambda + v_2)$ and $(30^\circ + v_1, 2.6\lambda + v_2)$, and two FF signals are located at $(5^\circ + v_1, +\infty)$ and $(-25^\circ + v_1, +\infty)$, where v_1 and v_2 are chosen randomly and uniformly within $[-1^\circ, 1^\circ]$ and $[-0.1\lambda, 0.1\lambda]$ in each trial, respectively. The SNR varies from 0 dB to 20

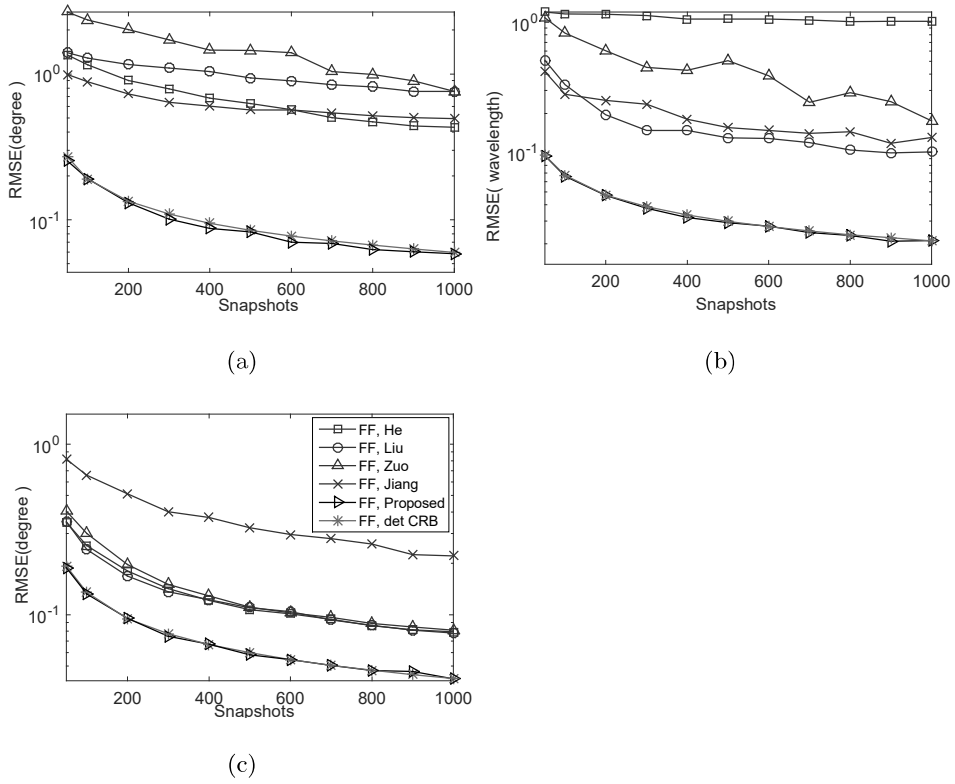

Fig. 3: RMSE of two NF and two FF sources versus snapshots number with SNR to be 10dB. (a) NF angle estimation. (b) NF range estimation. (c) FF angle estimation.

dB, with the number of snapshots fixed at 500. The RMSEs of the DOA and range estimates for NF signals and the DOA estimates for FF signals as a function of SNR are shown in Fig.2, respectively. From the results, we can see that the proposed method outperforms consistently the other four methods for both azimuth and range estimations. This is because the proposed method exploits the noncircular information of mixed signals, which increases the virtual array aperture to some extent. Furthermore, as SNR varies, the results of the proposed method follow closely the deterministic CRBs in (47).

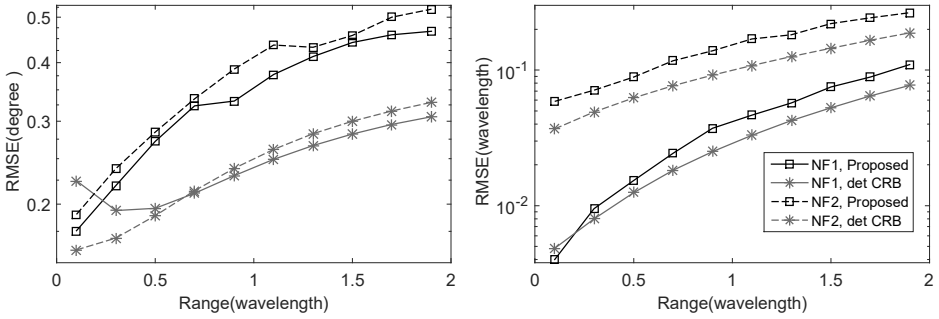

(a) (b)

Fig. 4: RMSE of two NF sources versus range with SNR to be 10dB and snapshots number to be 500. (a) NF angle estimation. (b) NF range estimation.

In the second set of simulations, we assess the performance of the proposed method versus the number of snapshots. The simulation conditions are similar to those in the first example, except that the SNR is set at 10dB, and the number of snapshots varies from 50 to 1000. The proposed method is compared with the four methods as in the first set of simulations in terms of the number of snapshots. In addition, the theoretical results as well as the deterministic CRBs are included as benchmarks. The results are presented in Fig.3. As expected, the RMSEs of the proposed method decrease as the number of snapshots increases, and they are much lower than that of the existing methods and also closer to the benchmark.

In the third set of simulations, we illustrate the performance of the proposed method versus variable ranges with a five-sensor ULA. Consider two pure NF signals incident from $(15^\circ + v_1, 0.3\lambda + \delta r)$ and $(30^\circ + v_1, 1.3\lambda + \delta r)$, where δr varies from 0.1λ to 1.9λ. The SNR is 10dB and the number of snapshots is 500. The resulting performance of the proposed method for DOA and range estimation is shown in Fig. 4(a) and Fig. 4(b). Clearly,

both the RMSEs and the CRB of DOAs and corresponding ranges of the NF sources are sensitive to the varied ranges. In addition, the RMSEs of DOA and range of the first NF are smaller than that of the second NF as the second source is far from the array, which is in accordance with the theoretical analyses in [10].

6. Conclusion

An effective localization method for a mixture of NF and FF rectilinear sources has been proposed, based on a symmetric ULA structure and the three-stage RARE principle, which avoids the direct 3-D peak-spectrum search. By exploiting the extended array manifold, the noncircularity property of the mixed sources is incorporated into the proposed method to increase the array aperture to some extent, which improves the estimation accuracy effectively. The deterministic CRB of the mixed NF and FF rectilinear signals are derived. Simulation results have shown the effectiveness of the proposed method as compared to that of all the considered existing methods.

Acknowledgement

This work is sponsored by Zhejiang Provincial Natural Science Foundation of China, and by Natural Science Foundation of Ningbo Municipality under Grant No. 2018A610094, and by National Natural Science Foundation of China under Grant No. 61628101 and 61571250, and by K.C.Wong Magna Fund in Ningbo University.

[1] H. Krim and M. Viberg, "Two decades of array signal processing re-

search: The parametric approach," *IEEE Signal Process. Mag.*, vol. 13, no.4, pp. 67-94, 1996.

[2] S. Qin, Y. D. Zhang, and M. G. Amin, "DOA estimation of mixed coherent and uncorrelated targets exploiting coprime MIMO radar," *Digit. Signal Process.*, vol. 61, pp. 26-34, Feb. 2017.

[3] X. F. Zhang, L. Y. Xu, L. Xu and D. Z. Xu, "Direction of departure (DOD) and direction of arrival (DOA) estimation in MIMO radar with reduced-dimension MUSIC," *IEEE Commun. Lett.*, vol. 14, no. 12, pp. 1161-1163, Dec. 2010.

[4] X. Wu, W.-P. Zhu, and J. Yan, "A Toeplitz covariance matrix reconstruction approach for direction-of-arrival estimation," *IEEE Trans. Veh. Technol.*, vol. 66, no. 9, pp. 8223-8237, Sep. 2017.

[5] Z.Q. He, Z. P. Shi, and L. Huang, "Covariance sparsity-aware DOA estimation for nonuniform noise," *Digit. Signal Process.*, vol. 28, pp. 75-81, May 2014.

[6] C. Zhou, Y. Gu, X. Fan, Z. Shi, G. Mao and Y. D. Zhang, "Direction-of-arrival estimation for coprime array via virtual array interpolation," *IEEE Trans. Signal Process.*, vol. 66, no. 22, pp. 5956-5971, Nov. 2018.

[7] J.W. Tao, L. Liu, and Z.Y. Lin, "Joint DOA, range, and polarization estimation in the Fresnel region," *IEEE Trans. Aerosp. Electron. Syst.*, vol. 47, no. 4, pp. 2657-2672, Oct. 2011.

[8] J. He, M. O. Ahmad, and M. N. S. Swamy, "Near-Field localization

of partially polarized sources with a cross-dipole array," *IEEE Trans. Aerosp. Electron. Syst.*, vol. 49, no. 2, pp. 857-870, Apr. 2013.

[9] J.Liang, X.Zeng, B. Ji, et al." A computationally efficient algorithm for joint range-DOA-frequency estimation of near-field sources," *Digit. Signal Process.*, vol. 19, no. 4, pp. 596-611, Jul. 2009.

[10] J. Liang and D. Liu, "Passive localization of mixed near-field and far-field sources using two-stage MUSIC algorithm," *IEEE Trans. Signal Process.*, vol. 58, no. 1, pp. 108-120, Jan. 2010.

[11] B. Wang, J. Liu and X. Sun, "Mixed sources localization based on sparse signal reconstruction," *IEEE Signal Process. Lett.*, vol. 19, no. 8, pp. 487-490, Aug. 2012.

[12] Y. Tian, Q.S. Lian, H. Xu, "Mixed near-field and far-field source localization utilizing symmetric nested array," *Digit. Signal Process.*, vol.73, pp. 16-23, Feb. 2018.

[13] B. Wang, Y. Zhao and J. Liu, "Mixed-order MUSIC algorithm for localization of far-field and near-field sources," *IEEE Signal Process. Lett.*, vol. 20, no. 4, pp. 311-314, Apr. 2013.

[14] Z. Zheng, J. Sun, W. Q. Wang, et al. "Classification and localization of mixed near-field and far-field sources using mixed-order statistics," *Signal Process.*, vol.143, pp.134-139, Feb.2018.

[15] J. He, M. N. S. Swany, and M. O. Ahmad, "Efficient application of music algorithm under the coexistence of far-field and near-field sources," *IEEE Trans. Signal Process.*, vol. 60, no. 4, pp. 2066-2070, Apr. 2012.

[16] J. J. Jiang, F. J. Duan, J. Chen, Y. C. Li and X. N. Hua, "Mixed near-field and far-field sources localization using the uniform linear sensor array," *IEEE Sensors J.*. vol. 13, no. 8, pp. 3136-3143, Aug. 2013.

[17] W. Zuo, J. Xin, J. Wang, et al. "A computationally efficient source localization method for a mixture of near-field and far-field narrowband signals," in *Proc. IEEE Int. Conf. Acoust., Speech, Signal Process. (ICASSP)*, Florence, 2014, pp. 2257-2261.

[18] G. Liu and X. Sun, Efficient method of passive localization for mixed far-field and near-field Sources, *IEEE Antennas Wireless Propag. Lett.*, vol. 12, pp. 902-905, 2013.

[19] G. Liu and X. Sun, "Spatial differencing method for mixed far-field and near-field sources localization," *IEEE Signal Process. Lett.*, vol.21, pp. 1331-1335, 2014.

[20] H. Abeida, J.P. Delmas, "Statistical performance of MUSIC-like algorithms in resolving noncircular sources," *IEEE Trans. Signal Process.*, vol. 56, no. 9, pp. 4317-4329, Sep. 2008.

[21] H. Chen, C. P. Hou, W. P. Zhu, et al. "ESPRIT-like two-dimensional direction finding for mixed circular and strictly noncircular sources based on joint diagonalization," *Signal Process.*, vol.141, pp.48-56, Dec.2017.

[22] J. Steinwandt, F. Roemer, M. Haardt, et al. "Performance analysis of multi-dimensional ESPRIT-type algorithms for arbitrary and strictly non-circular sources with spatial smoothing," *IEEE Trans. Signal Process.*, vol. 65, no. 9, pp. 2262-2276, May 2017.

[23] Y. Shi, L. Huang, C. Qian, et al. "Direction-of-arrival estimation for noncircular sources via structured least squares-based esprit using three-axis crossed array," *IEEE Trans. Aerosp. Electron. Syst.*, vol. 51, no. 2, pp. 1267–1278, 2015.

[24] H. Abeida, J.P. Delmas, "MUSIC-like estimation of direction of arrival for non-circular sources," *IEEE Trans. Signal Process.*, vol. 54, no. 7, pp. 2678-2690, Jul.2006.

[25] H. Huang, B. Liao, Guo X, et al. "DOA estimation of rectilinear signals with a partly calibrated uniform linear array," *Signal Process.*, vol.147, pp.203-207, Jun.2018.

[26] Z. M. Liu, Z. T. Huang, Y. Y. Zhou , et al. "Direction-of-Arrival estimation of noncircular signals via sparse representation," *IEEE Trans. Aerosp. Electron. Syst.*, vol. 48, no. 3, pp. 2690-2698, Jul. 2012.

[27] J. Liu, Z.T. Huang and Y.Y. Zhou, "Extended 2q-MUSIC algorithm for noncircular signals," *Signal Process.*, vol. 88, no. 6, pp. 1327-1339, Jun. 2008.

[28] H. Abeida and J. P. Delmas, "Direct derivation of the stochastic CRB of DOA estimation for rectilinear sources," *IEEE Signal Process. Lett.*, vol. 24, no. 10, pp. 1522-1526, Oct. 2017.

[29] H. Chen, C. P. Hou, W. Liu, et al. "Efficient two-dimensional direction of arrival estimation for a mixture of circular and noncircular sources," *IEEE Sensors J.*, vol. 16, no. 8, pp. 2527-2536, Apr. 2016.

[30] J. Steinwandt, F. Roemer, M. Haardt, et al. "Deterministic cramér-rao bound for strictly non-circular sources and analytical analysis of

the achievable gains," *IEEE Trans. Signal Process.*, vol. 64, no. 17, pp. 4417- 4431, Sep. 2016.

[31] B. Liao, Z. G. Zhang and S. C. Chan, "DOA estimation and tracking of ULAs with mutual coupling," *IEEE Trans. Aerosp. Electron. Syst.*, vol. 48, no. 1, pp. 891-905, Jan. 2012.

[32] A. Ferreol, E. Boyer and P. Larzabal, "Low-cost algorithm for some bearing estimation methods in presence of separable nuisance parameters," *Electron. Lett.*, vol. 40, no. 15, pp. 966-967, Jul. 2004.

[33] M. Pesavento, A. B. Gershman and K. M. Wong, "Direction finding in partly calibrated sensor arrays composed of multiple subarrays," *IEEE Trans. Signal Process.*, vol. 50, no. 9, pp. 2103-2115, Sep. 2002.

[34] J. Xie, H. Tao, X. Rao, et al. "Comments on near-field source localization via symmetric subarrays," *IEEE Signal Process. Lett.*, vol. 22, no. 5, pp. 643-644, May 2015.

[35] L. Wan and L. Xie, "An improved DOA estimation algorithm for circular and non-circular signals with high resolution," in *Proc. IEEE Int. Conf. Acoust., Speech, Signal Process. (ICASSP)*, Shanghai, 2016, pp. 3051-3055.

[36] H. Gazzah and J.P. Delmas, "CRB Based-design of linear antenna arrays for near-field source localization," *IEEE Trans. Antenna Propag.* , vol. 62, no. 4, pp. 1965-1973, Apr.2014.

[37] Y. Begriche, M. Thameri, and K. Abed-Meraim, "Exact conditional and unconditional Cramer-Rao bound for near field localization," *Digital Signal Process.*, no. 31, pp. 45-58, Aug. 2014.

[38] J.P. Delmas, H. Abeida, "Stochastic Cramer-Rao bound for non-circular signals with application to DOA estimation," *IEEE Trans. Signal Process.*, vol. 52, no. 11, pp. 3192-3199, Nov. 2004.